Urban Heat Island Effects and Thermal Comfort in Abuja Municipal Area Council of Nigeria

*Isioye, O. A., Ikwueze, H. U. and Akomolafe, E. A.
Department of Geomatics, Ahmadu Bello University, Zaria –Nigeria.
*Correspondence email: lekkyside4u@yahoo.com

Abstract

Climate change is a global challenge with multiple consequences. One of its impacts is the increase in surface temperature intensity. The hazard is higher for populaces living in urban areas, where the most elevated temperatures are commonly recognized, because of the Urban Heat Island (UHI) effect. The city of Abuja in recent times has experienced an increase in both surface and atmospheric temperatures. In this study, an evaluation of the ecological impact of UHI effect of Abuja Municipal area was conducted using Landsat 8 data of 2019. The surface temperature of the city was estimated and evaluated using its thermal-infrared (TIR) band (10.40µm – 12.50µm). Furthermore, the correlation between LST and Normalized Difference Vegetation Index (NDVI) as well as the Normalized Difference Build-Up Index (NDBI) was also assessed to validate the accuracy of the LST. The urban thermal field variance index (UTFVI) was applied to measure the thermal comfort level of the city, which quantitatively assessed the UHI impacts on the nature of urban life. Results show that the LST of Abuja city ranges from approximately 19°C to 39°C with the UHI observed in the northern and eastern parts of the city. The UTFVI map associated with UHI indicates that the outer peripheries of the city are ecologically more comfortable than the inner segments. In general, 40% of the city experiences ecologically bad or worse UHI effects, indicating a need for continued UHI mitigation efforts.

Keywords: Urban Heat Island (UHI), Land surface temperature (LST), Urban Thermal Field Variance Index (UTFVI), Normalized Difference Vegetation Index (NDVI), Landsat OLI/TIRS

INTRODUCTION

Rising temperatures due to global climate change is amplified by the effect of urban heat islands (Della-Marta, *et al.*, 2017). This phenomenon is widely analyzed and is one of the major themes of urban climatology, particularly its impact on human health (Huang and Lu, 2018). With more than half of the world's people living in urban areas (55%, up from 30%), urbanization determines the spatial distribution of the world's population and is one of the four demographic mega-trends, with the growth of the global population, population ageing, and international migration (World Urbanization Prospects, 2019). There is a predictable change in the urban environment as a consequence of this growth. One such change in urban climates particularly is the formation of Urban Heat Islands (UHI), a situation where the cities' or metropolitan areas' ambient temperature is dramatically altered and become warmer than the surrounding rural areas (Oleson, *et al.*, 2005; Gago, *et al.*, 2013; Alfraihat *et al.*, 2016).

The Urban Heat Island (UHI) is a phenomenon that affects millions of people worldwide. The UHI affects urban quality of life through its impacts on human health, ecosystem function, local weather and climate. There is a direct relationship between peak UHI intensity and heat-related illness and fatalities (Oleson, *et al.*, 2005; U.S. EPA, 2014; Alfraihat *et al.*, 2016).

In several literatures across the globe, built-up areas and bare land have been shown to accelerate the effect of UHI, whereas green space and water reduce the UHI intensity (Amiri *et al.*, 2009). Furthermore, a complex pattern of landscape composition and configuration controls LST (Zhou *et al.*, 2014; Asgarian *et al.*, 2015) while some researches opined that natural and socioeconomic factors simultaneously create certain effects on the LST form (Jenerette *et al.*, 2007; Buyantuyev and Wu, 2010;). In addition, diurnal variation in different seasons plays a major role in identifying the impact and expansion of UHI in any particular city region because daytime LST is more unstable than nighttime LST (Zhou *et al.*, 2013; Guha *et al.*, 2017).

In Nigeria, just like many other African countries, the capital cities are often faced with the problem of rapid urbanization, which from the aforesaid contributes majorly to the UHI intensity. Over time, the city of Abuja has experienced a high rate of population growth and urbanization (Adeyeri *et al.*, 2015). According to census data, from 1991 and 2006, the population of Abuja has been steadily growing since the relocation of Nigeria’s capital from Lagos. It has grown phenomenally from a population of 113,000 in 1976, 378,671 in 1991 to 1.4 million in 2006 (NPC, 2006). In a 2017 study undertaken by the Federal School of Surveying and the Federal Capital Development Authority (FCDA), Abuja’s population growth was estimated at 8.32% per annum, while satellite city populations were found to be rising even more quickly, at an estimated 20% each year. Rapid urbanization can be attributed to a range of factors including better economic opportunities on offer in the territory, underinvestment in smaller towns and villages surrounding the FCT, and the relative safety of the area in a region affected by pockets of conflict. A greater part of this population, due to inadequate accommodation and high rents in the city, end up settling in the suburbs of the city; in areas such as Kubwa, Karu, Masaka, and Nyanya. The urban growth rate of suburbs such as Karu and Nyanya in 2001 was 66.2% compared to Abuja city which was 40.2% (Jinadu, 2004).

Urban growth in Abuja has been sped up, and extreme stress to the environment has occurred. This is particularly true in the city where massive agricultural land is disappearing each year, converting to urban or related uses. Land transformation due to urbanization has also caused noticeable climate changes, including increased energy demands and air pollution thereby impacting the quality of urban life (Gray, *et al., 2000*; Alfraihat *et al.*, 2016). The impact of this rapid urbanization is already being felt in Abuja city as the surface temperature progressively spikes yearly. According to Aljazeera (2019), the months of March, April and May 2019 experienced extreme heat, with the Nigerian Meteorological Agency (NiMET) saying that the rise in temperature has been affecting most parts of the country, including coastal areas, with temperatures well above 35^{o}C.

Furthermore, variables derived from remote sensing and meteorology have been combined to explain UHI phenomenon in Abuja city environment and the varying importance of time of the day on overall efficiency of the city's UHI mitigation efforts have been reported (Adebayo *et al.*, 2015; Alfraihat *et al.*, 2016). However, a spatially-resolved ecological evaluation UHI effects with an Urban Thermal Field Variance Index (UTFVI) is pending for the city of Abuja city. With the urbanization growing rapidly, the ecological assessment of UHI has become important as it influences development and human living environment (Chen *et al.,* 2006; Mackay, 2012; Isioye *et al.*, 2019). Meanwhile, increasing urban heat in Abuja city municipal area presents a noticeable health risk for the growing population and are likely to escalate the stress or discomfort arising from the heat.

From the aforementioned, this study seeks to use remotely sensed surface temperature data to retrieve LST of the study area for the year 2019 and analyze the city's UHI phenomenon, and carry out an UTFVI assessment to appraise level of thermal comfortability within the different areas of the city of Abuja. In this paper, the different data sets used in the study and procedures for estimation of UHI and UTFVI are presented in Section 2. In Section 3, the results are presented and discussed. The summing up and concluding remarks are given in the final part.

Description of the study area

The city of Abuja is located in central Nigeria in the Guinea savanna between Latitudes 8°25'N and 9°25'N and Longitudes 6°45"E and 7°45'E and occupies an area of about 8,000 square kilometers. Abuja was built in the 1980s before it officially became the capital city of Nigerian in 1991. The 2006 census showed that the population of Abuja was776, 298 people (NPC, 2006). In 2015, the city had an annual growth of at least 35%, making it the fastest-growing city in Africa and one of the fastest in the world (Abuja Facts, 2015).

The Köppen climate classification for Abuja features a tropical wet and dry climate. The weather conditions include a warm, humid rainy season and a blistering dry season. The rainy season starts in April and ends in October yearly. The annual rainfall is about 1,631.7mm and the annual mean temperature ranges between 25.8°C and 30.2°C (Balogun, 2001). Abuja is located at about 840m above mean sea level and this coupled with undulating terrain of the study area act as a moderating influence on its weather.

Abuja has witnessed a remarkable rural-urban migration of people, causing alterations and modifications in the LULC which has led to the development of satellite towns to which the city is sprawling. Due to this, more vegetal covers are being converted to urban infrastructure and result in micro-climate change and UHI growth. A map of the study area is shown in the Figure 1.

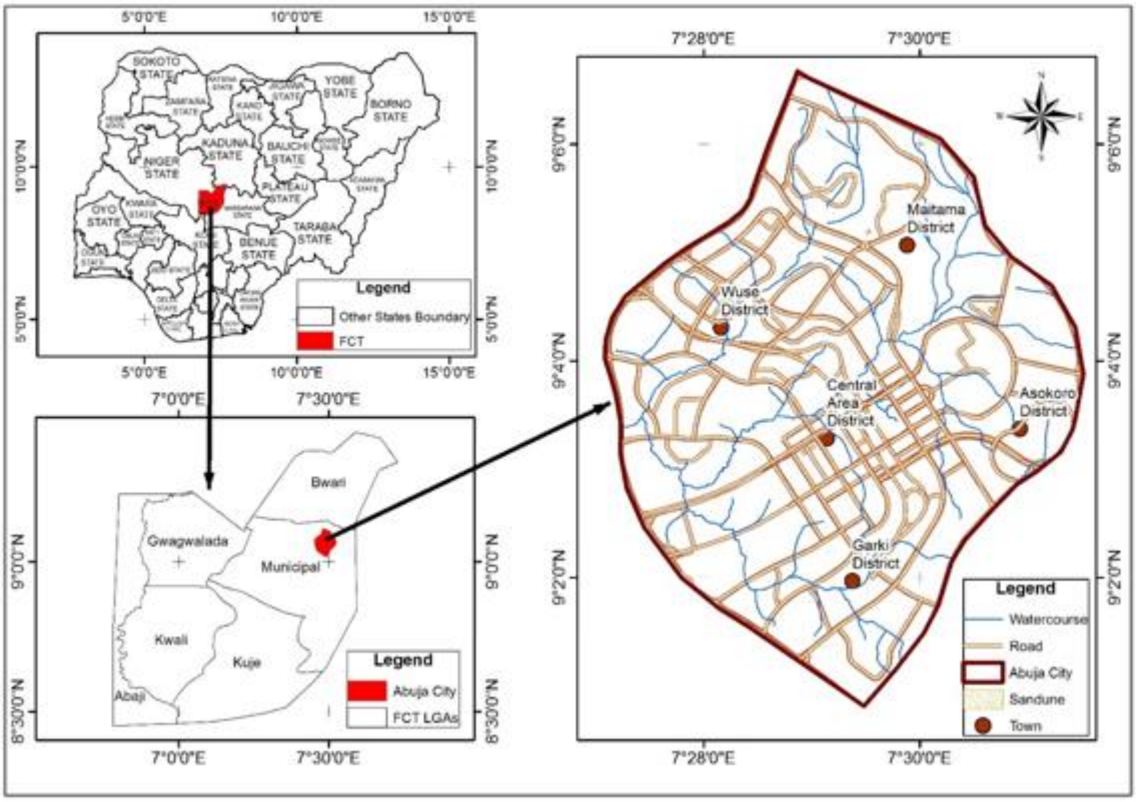

Figure 1. Map of the study area; Abuja city

DATA AND METHOD

Data

Basically, satellite and methodological data were required to conduct this research. Landsat satellite images were obtained from the U.S. Geological Survey (USGS) earth explorer website via https://earthexplorer.usgs.gov/. The images selection was based on their good quality mainly in terms of cloud cover, date, month and year of collection (See Table 1). USGS supplies image(s) after geo-referencing them to the Universal Transverse Mercator (UTM), map projection (Zone 32), WGS 84 datum and ellipsoid. The detailed descriptions of the satellite images selected are shown in Table 1.

Table 1. Specifications of the satellite data used

S/N	Satellite	Sensor	Path/Row	Acquisition date	Spatial resolution	Cloud cover
1	Landsat 7	ETM+	189/54	03/12/2009	30m/60m	0%
2	Landsat 8	OLI/TIRS	189/54	15/12/2019	30m/100m	0%

Weather records corresponding to the same time the LANDSAT image was acquired are needed for the algorithms used to derive the LST and the UTFVI. These weather data include relative humidity, dew points, and atmospheric temperature of the study area. The weather data were acquired from The Weather Channel Interactive Inc. website via http://www.wunderground.com/. Additionally, water vapor content in the air was among the required parameters for the UTFVI retrieval for ecological evaluation. The water vapor content was calculated as a function of Relative Humidity (RH) and near surface temperature (T_o) (Zhang *et al.*, 2013; Alfraihat *et al.*, 2016).

Method

The mono-window algorithm, the split-window algorithm, temperature-emissivity separation algorithm and the single-channel method (Gillespie *et al.*, 1998; Jimenez-Munoz, *et al.*, 2003; Lia, *et al.*, 2013) are some of the several algorithms available for retrieving LST, a key parameter for the UHI estimation. While the split-window and temperature-emissivity separation algorithms are primarily developed for the Advanced Spaceborne Thermal Emission and Reflection Radiometer (ASTER) data, both the mono-window and single-channel algorithms are applicable for thermal LANDSAT data, of which the mono-window algorithm is relatively simple and highly effective for retrieving the LST for the analysis of the UHI (Liu, *et al.*, 2011; Alfraihat *et al.*, 2016).

To effectively appraise the ecological impact of UHI effect on Abuja municipal area, three fundamental steps were followed. These include:

a) Deriving a Normalized Difference Vegetation Index (NDVI) and a Normalized Difference Built-up Index (NDBI);
b) Retrieving the LST and analyzing the city's UHI phenomenon; and
c) Calculating the Urban Thermal Field Variance Index (UTFVI) and interpreting the ecological valuation of the UHI impacts.

The Normalized Difference Vegetation Index (NDVI)

The Normalized Difference Vegetation Index (NDVI) is calculated from the visible red and near infrared bands. The rationale of the index is that healthy vegetation has a high reflectance in the near infrared (NIR) and a low reflectance in the red, thereby enhancing the interpretation of vegetation cover while suppressing subtle noise from other land cover types. The NDVI can be calculated as using equation (1).

$$NDVI = \frac{NIR - RED}{NIR + RED} \tag{1}$$

In equation (1), NIR and RED in Landsat images are the reflectance in the near-infrared and visible red portion of Electromagnetic spectrum respectively. In this study, the NDVI is calculated for two fundamental reasons, i.e., understanding the city's vegetation pattern and extracting emissivity values.

First, the NDVI values indicate whether the land cover type is vegetation, which has been shown to have a cooling effect on surfaces temperatures, hence adopted as the UHI mitigation strategies. Secondly, the NDVI was also used to derive emissivity values from the LANDSAT data based on their mutual direct relationship. The emissivity values are critical parameters needed for modeling the LST from the LANDSAT 8 OLI image.

The Normalized Difference Built-up Index

The Normalized Difference Built-up Index (NDBI) has been an effective technique to map built-up areas with accuracy of 92% (Zha *et al.*, 2005, Alfraihat *et al.*, 2016). The index is calculated from reflectance bands of Landsat 8 image as:

$$NDBI = \frac{Band6 - Band5}{Band6 + Band5} \tag{2}$$

Retrieving the Land Surface Temperature (LST)

Band 10 of Landsat 8 OLI 8 image is a thermal-infrared (TIR) band that has been commonly used for the LST mapping. The following steps were executed in this study in order to retrieve the LST of the study area.

Conversion of DN to spectral radiance

To retrieve the LST, the Landsat data were first radiometrically corrected by converting the digital numbers (DN) of each band to spectral radiance. It has been proven that radiation correction improves the accuracy of LST and other index calculation (Song *et al.*, 2001). This was achieved in ENVI (an image processing software) using the following equation (Landsat Project Science Office, 2016):

$$L_\lambda = M_L \times QCal + A_L, \tag{3}$$

In equation (3), L_λ is TOA spectral radiance in Watt/(m^2srμm), M_L is the band-specific multiplicative rescaling factor from the metadata (RADIANCE_MULT_BAND 10 for Landsat 8 OLI/TIRS), QCal is the quantized and standard product pixel value (DN), A_L is the band-specific additive rescaling factor from the metadata (RADIANCE_ADD_BAND 10 for Landsat 8 OLI/TIRS).

Conversion of spectral radiance to TOA brightness temperature

The spectral radiance converted from pixel DN values above was used to compute Top of Atmosphere brightness temperature (T_B) which is the effective temperature viewed by the satellite under an assumption of unit emissivity in Kelvin. The brightness temperature was computed using the following equation (Avdan and Jovanovska, 2016):

$$T_B = \frac{K_2}{ln\left(\frac{K_1}{L_\lambda} + 1\right)} \tag{4}$$

In equation (4), K_1 and K_2 = band specific thermal conversion constant. For Landsat 8 OLI, K_1 = 774.89 mW/cm^2/sr/μm and K_2 = 1321.08 Kelvin.

Estimation of proportion of vegetation and emissivity

Alemu (2019), defined land surface emissivity as the “ratio of energy emitted from a natural material to that of a perfect emitter (blackbody) at the same temperature”. Land surface emissivity (LSE) can be derived from the emitted radiance measured from space. Land surface emissivity is the average emissivity of an element of the surface of the Earth calculated from NDVI values. The proportion of vegetation (Pv) is computed as follows:

$$Pv = \left[\frac{(NDVI - NDV\,Im\,i\,n)}{(NDV\,Im\,a\,x - NDV\,Im\,i\,n)}\right]^2 \tag{5}$$

Where, Pv = Proportion of vegetation, NDVI = NDVI Values from the Image, NDVImin = Minimum NDVI, and NDVImax = Maximum NDVI. Using the computed value of proportion of vegetation (Pv) the Land Surface Emissivity (e) was computed as follows:

$$e = 0.004 * P_v + 0.986 \tag{6}$$

Land Surface Temperature (LST) retrieval

The following equation were used for the conversion from at-satellite temperature to land surface temperature in Celsius.

$$LST(^oC) = \frac{T_B}{\left[1 + \left(\lambda \times \frac{T_B}{\rho}\right) ln(e)\right]} - 273.15 \tag{7}$$

In equation (7), λ is the wavelength of emitted radiance, ρ = h×(c/s) = 1.4388 × 10^{-2}m K = 14388 µm K, h is the plank's constant = 6.626 × 10^{-34}Js, s is the Boltzmann constant = 1.38 × 10^{-23}J/K, c = velocity of light = 2.998 × $10^8 m/s$. For obtaining the results in Celsius, the radiant temperature is revised by adding the absolute zero (approx. -273.15^{o}C).

Extraction of water vapor content

The atmosphere's water vapor content was derived from the relative humidity (RH) and the near-surface temperature. Water vapor content can be estimated by the following equation:

$$w = 0.0981 \times \left\{10 \times 0.6108 \times exp\left[\frac{17.27 \times (T_o - 273.15)}{273.3 + (T_o - 273.15)}\right] \times RH\right\} + 0.1697, \tag{8}$$

where w is the water vapor content (g⁄cm^2), T_0 is the near-surface air temperature in Kelvin (K), and RH is the relative humidity (%).

Extraction of atmospheric transmittance

There is a difference between values of at-sensor and ground temperatures, because of the attenuation caused by the atmosphere. Hence, the atmospheric transmittance is calculated to account for this attenuation.

Once the water vapor content was calculated, the atmospheric transmittance was estimated with the following equation (Qin *et al.*, 2001; Lia, *et al.*, 2013; Alfraihat *et al.*, 2016) in Table 2.

$$\tau = 1.031412 - 0.11536w \tag{9}$$

where τ is the total atmospheric transmittance and *w* is the water vapor content.

Table 2. Atmospheric transmittance as a function of Water Vapor Content of the Air column (profile) for four standard atmospheric conditions.

Air Column (Profile)	Water vapor content (w) (g/cm^2)	Atmospheric Transmittance Equation
High air temperature	0.4 – 1.6	$\tau = 0.974290 - 0.080076w$
High air temperature	1.6 – 3.0	$\tau = 1.031412 - 0.11536w$
Low air temperature	0.4 – 1.6	$\tau = 0.982007 - 0.09611w$
Low air temperature	1.6 – 3.0	$\tau = 1.053710 - 0.14142w$

Finally, the mean atmospheric temperature (T_a) was estimated from near surface air temperature based on regional conversion formula proposed (Qin *et al.*, 2001; Sun *et al.*, 2010) (See Table 3).

Table 2. Effective mean atmospheric temperature for four standard atmospheres.

Standard atmosphere	Effective mean atmospheric temperature (T_a) (K)
For USA 1976	$T_a = 25.9396 + 0.88045T_0$
For tropical	$T_a = 17.9769 + 0.91715T_0$
For mid-latitude summer	$T_a = 16.0110 + 0.92621T_0$
For mid-latitude winter	$T_a = 19.2704 + 0.91118T_0$

The near surface temperature in degree Kelvin is Abuja city air temperature recorded at the time of satellite overpass. Accordingly, since Abuja is located in the tropical region, the mean aerial temperature of Abuja city was given by:

$$T_a = 17.9769 + 0.91715T_0, \tag{10}$$

where T_a is the mean atmospheric temperature and T_0 is the near-surface air temperature.

Model Validation

The NDBI and NDVI were used for the verification of the modeled LST values. Both qualitative and quantitative validation methods are used for verification. Qualitatively, visual interpretations and comparisons of the images of the NDBI, NDVI and LST values were done and correlation matrix was used for the quantitative evaluation. Theoretically, the LST values must have a positive relationship with the NDBI values and a negative relationship with the NDVI values.

The Urban Thermal Field Variance Index

In this study, the UTFVI was used for the ecological evaluation of Abuja city's urban heat island because of its prior tested application to Landsat data. The UTFVI values were classified into six categories, each having corresponding interpreted ecological valuations and the UHI phenomenon (Liu and Zhang, 2011; Alfraihat *et al.*, 2016). The index, which analyzes the UHI effect on the quality of urban life, is calculated using equation (11) as follows:

$$UTFVI = \frac{T_S - T_{mean}}{T_{mean}}, \qquad (11)$$

where UTFVI is the urban thermal field variance index, T_s is the LST (°C), and T_{mean} is the mean LST (°C).

RESULTS AND DISCUSSION

The Accuracy Validation of LST Retrieval

The LST of the study area was calculated from Landsat 7 and 8 images for the years 2009 and 2019 respectively. These maps were generated to compute the mean surface temperature over a 10-year period and to observe changes in the temperature over time. The retrieved LST maps are shown in Figure 2.

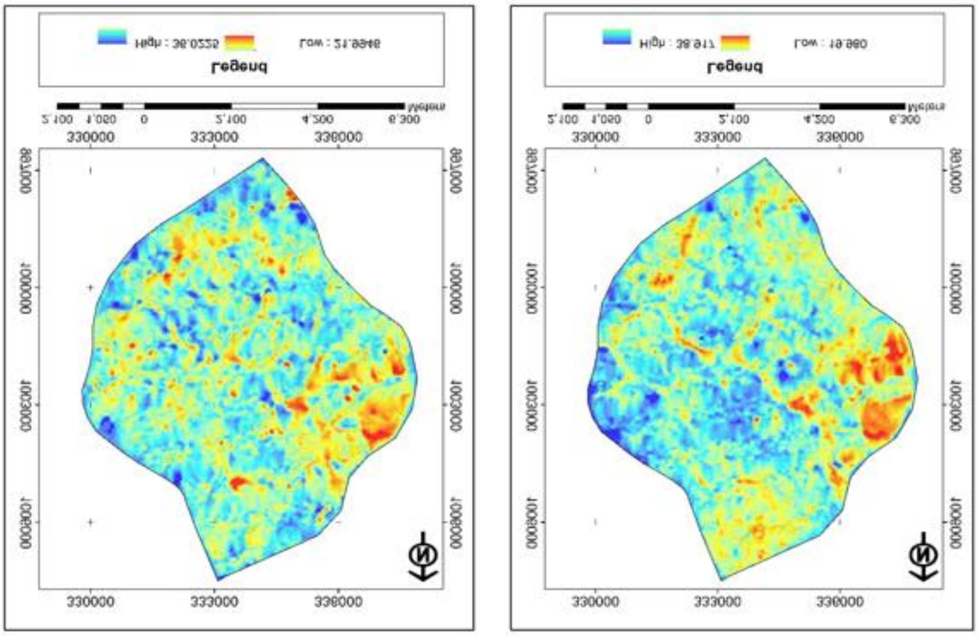

Figure 2. LST distribution maps derived from Landsat images of (a) 2009 and (b) 2019

The visual interpretation of the images of the NDBI, NDVI and LST values substantiated the theoretical relationship between these variables (Figure 3). Expanses with the high NDVI values (e.g., grassland) have low NDBI values and low LST. On the other hand, waterbodies while having low NDVI values (NDVI< 0), also have low LST and NDBI values. As expected, built-up areas have high NDBI values with low NDVI values and high LST (LST > 35°C).

As shown in Table 3, the quantitative evaluations of the LST, NDBI and NDVI images, through correlation matrix, also showed similar outcomes. There exist a strong negative correlation between NDVI and NDBI (r = -0.7337). The high negative correlation between the NDBI and NDVI images is indicative of declining vegetation cover as more built-up areas emerge as land use. Conversely, the relationship between the LST and NDBI images is a moderate positive correlation (r = 0.4075), indicating an increase in surface temperature as more land use/cover is converted to built-up while a moderate negative correlation is observed between LST and NDVI (r = -0.4547) for the area under study.

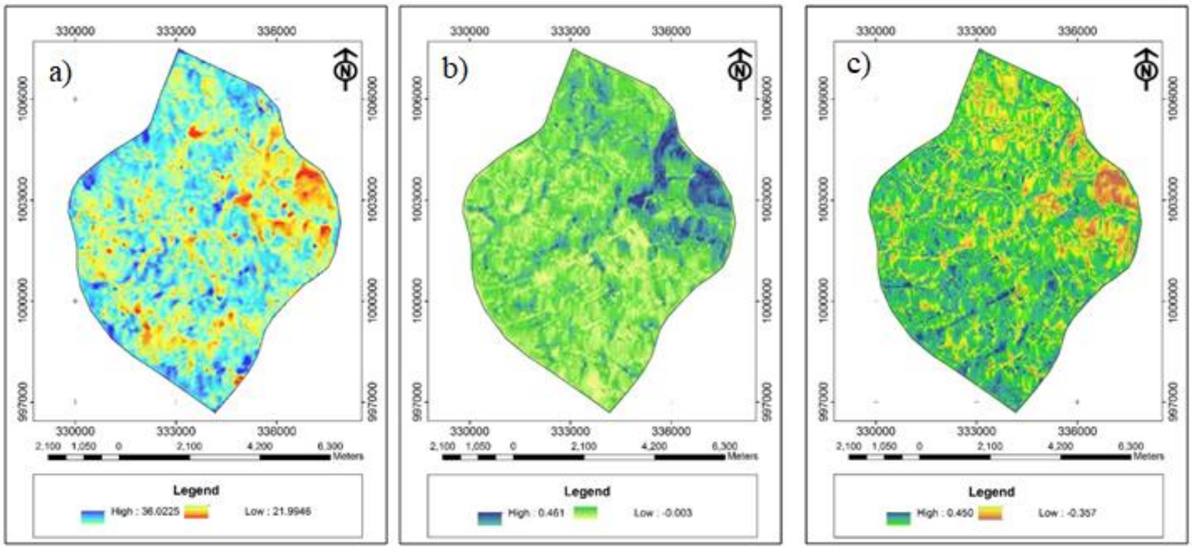

Figure 3. LST and corresponding NDVI and NDBI values of the study area, (a) LST map (b) NDVI map (c) NDBI map.

Table 3. Correlation matrix of LST, NDBI and NDVI of Abuja city after masking the water bodies

	LST	NDBI	NDVI
LST	1	0.40746	-0.45471
NDBI	0.40746	1	-0.7337
NDVI	-0.45471	-0.7337	1

The positive relationship which exist between LST and NDBI values reveals the heating impact of built-up and impervious surface areas on surface temperature, while the negative relationship of the LST and NDVI values ascertained the cooling impact of forests, woodlands, parks, and other city green spaces. The direction of the relationship captured by the correlation matrix is significant, as correlation matrix was generated through pixel-based comparison.

Several previous studies have shown a comparable relationship between the LST values and these indices (Gallo and Owen, 1998; Chen, *et. al*, 2006; Li *et. al*, 2010). It is not quite clear why the cooling effect of the natural vegetation decimates when the percent canopy cover increases. And yet the negative correlation between the NDVI and LST indicate the effect of vegetation in reducing the UHI effect, thereby reassuring its utility for UHI mitigation. On the other hand, the positive NDBI and LST relation (Chen *et. al*, 2006). indicated the logical association of the built-up areas and UHI. Both uncrowned settlement pattern, greening urban spaces and increasing the albedo (i.e., reflection coefficient) of the built-up surfaces can be adopted to lessen the impacts of the UHI in Abuja city.

Analysis of Urban Heat Islands (UHI) of Abuja city

The spatial distribution of the LST of Abuja city is shown in Figure 2. According to the result, the mean LST is 26.5°C, the maximum and minimum LSTs are 20°C and 33°C, respectively. The higher LST dominates northwestern and north central areas of the city, while the eastern, southern and extreme northern areas have the lower LST. The UHI impacts of built-up areas were found to depend on the density of settlement with medium sized building. In Abuja city, settlements in the south of the city are less populated and have visible green spaces as compared with areas to the north.

The results verify a previous Abuja UHI project (Adeyeri *et al.,* 2015) which reported a consistent high UHI intensity in northwestern Abuja city land as compared to the east and downtown area.

From the results it is observed that, a large portion of Abuja city (i.e., 49.5%) experiences LSTs of around 30 to 37°C. This was found mainly in areas around Wuse zone 2 to zone 4 and other populated residential areas. About 26.1% of the city, mainly in the north and northwestern areas constitute the second largest LST class (28 – 30°C) while the hottest LST class (i.e., 38°C and above) is experienced in relatively small pocket areas, covering about 5.2% of Abuja city, mainly where the large commercial buildings like markets and car parks are located. The high UHI is detected in large commercial and residential areas due to influx of people who come together to do business, board a vehicle or maybe indicating the possible air heating impacts of gases emitted from vehicles, building cooling systems and reflection or absorbance of roofing sheets. Areas having the LSTs between (22 - 27°C) constitute 10% of the landscape, and these are lands in close proximity to the parks, forest vegetation, woodlands and green spaces. However, the lowest LST (less than 22°C) is recorded in only 9.2% of the city; mainly on the lands covered by water (i.e., lakes and wetlands).

The Ecological Evaluation of Abuja city Urban Heat Islands

To reflect the changes of urban thermal field directly, UTFVI can be further divided into six levels in accordance with six different ecological evaluation indices (Zhang, 2006). Table 4 gives the specific thresholds in the six UTFVI levels while the quantitative ecological evaluation of the UHI effects in Abuja city is shown in Figure 3.

Table 4. The interpretation of the index quantitative evaluating of the ecological effects of the Abuja municipal area UHI (Qin *et al.*, 2001; Lia, *et al.,* 2016; Alfraihat *et al.*, 2016).

Urban Thermal Field Variance Index	Urban Heat Island phenomenon	Ecological Evaluation Index
Less than 0	None	Excellent
From 0 to 0.005	Weak	Good
From 0.005 to 0.01	Middle	Normal
From 0.01 to 0.015	Strong	Bad
From 0.015 to 0.02	Stronger	Worse
More than 0.02	Strongest	Worst

According to the Urban Thermal Field Variance Index (UTFVI), which measures urban ecological quality of life in terms of the degree of thermal comfort in relation to the existence of the UHI phenomenon, varying impacts of the UHI were detected in Abuja city. The city has the two extremes: areas of heat stresses (i.e., UTFVI > 0.02) and areas optimal microclimate (i.e., UTFVI <0) (Figure 4).

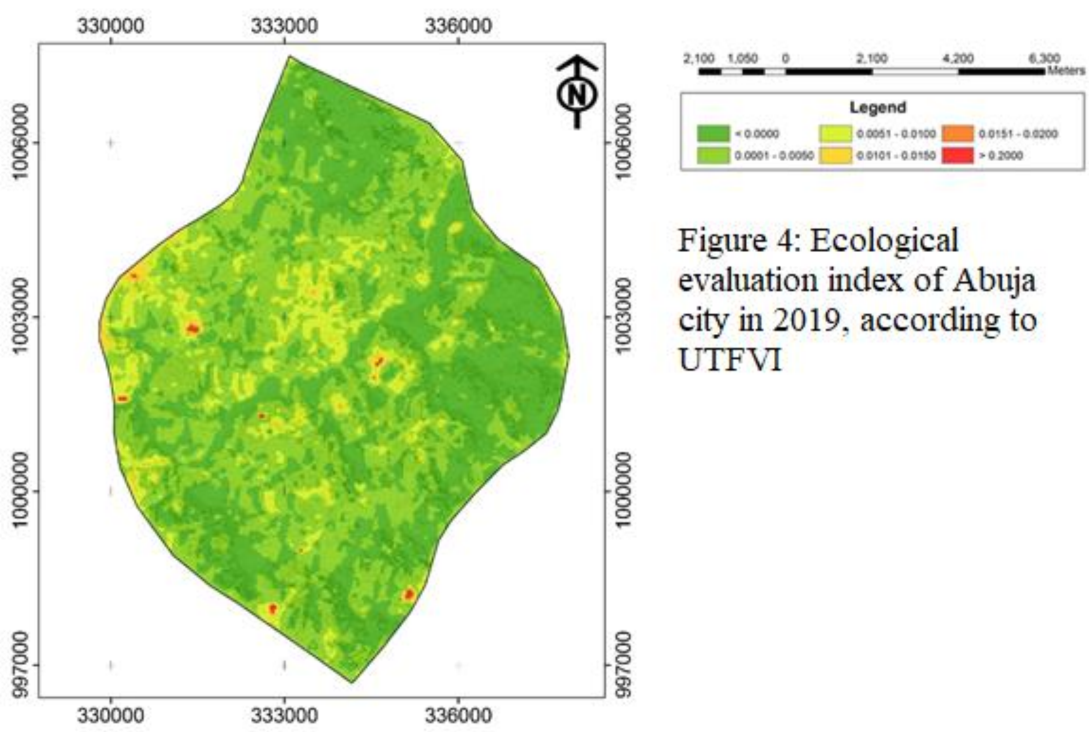

Figure 4: Ecological evaluation index of Abuja city in 2019, according to UTFVI

The largest portion of Abuja Municipal Area Council (44.18%) experiences optimal thermal condition (i.e., UTFVI <0) for living. These areas are located in the periphery of the city and locations in close proximity to the streams, wetlands, hills, woodlands, parks and green spaces. On the other hand, the areas that are hit by the worse UHI effects (i.e., UTFVI > 0.01) are relatively small pocket areas (i.e., 10.26%) of Abuja municipal area; while those experiencing thermal discomfort accounts for 11.25% of the study area. In general, according to the ecological evaluation of the UHI effects, the UTFVI did not detect thermal discomfort on 88.75% of the city. It was only in the remaining 11.25% of the city that varying degrees of thermal discomfort and heat stresses were detected.

In general, the UTFVI analysis of Abuja Municipal Area Council conforms to studies that analyzed spatiotemporal patterns of the UHI over Abuja using Landsat sensors. In a study carried out by Adeyeri *et al.* (2015), they observed that between 1987 and 2014, the LST rose by 7.66K with 2014 recording a mean LST of 309.05K while 1987 had a mean LST of 301.39. This shows that the change in the temperature of Abuja is quite significant and this could also affect the thermal comfort and health condition of the locals residing in Abuja city. The LST for the period of study was observed to be an increasing trend.

According to the report, even if there is a reduction in the UHI intensity, because of the city's UHI mitigation strategies, northeastern and pockets of areas in northern and southern of the study area are still experiencing the UHI stresses. Therefore, urban planning that pursues spacious settlement pattern with green spaces and parks, and wetlands preservation is important to strengthen Abuja city's UHI mitigation strategies and thereby to maintain urban quality of life.

CONCLUSION

Temperature and land cover interaction studies provide valuable insights for urban environment analysis as well as assistance in various city planning and decision-making processes for the city development. The results from this study indicate that changes in UTFVI distribution can be largely related to the expansion of urban area during the period under study (2009 – 2019). The LST, extracted from Landsat 8 OLI/TIRS imagery, Band 10, shows that the distribution of UHI I Abuja municipal area council (AMAC) varies. In general, results show that was a difference of 19°C between the low UHI intensity areas around the water body and the high UHI intensity areas in the densely populated northeastern neighbourhoods.

In addition, from the correlation analysis of the retrieved LST with NDVI and NDBI, it was found that that the green land can weaken urban heat island effect, but the built-up land can accelerate the effect. The distribution of the UHI phenomena were found to have a direct relationship to the city's land use/land cover distribution. While woodlands, urban parks and green spaces, have lowered the phenomena of UHIs; densely populated buildings, congested settlement, industrial zones and large train stations have intensified the UHI effects. Thus, this study recommends that in future city planning and development, more attention should be paid to urban greening.

Results obtained from the analysis to Abuja Municipal Area's Urban Thermal Field Variance Index (UTFVI), ranges of thermal comforts were detected. The hot spot of UTFVI were found mainly in the built-up areas especially densely populated district and in commercial districts of the city. These are likely areas that are susceptible to UHI. It was observed that 88.75% Seventy-two percent of the city's landscape experiences normal microclimate for living, which is encouraging. However, a bad-to-worse heat stress condition is detected in sizable portion of the city (11.25%), indicating potential impacts of the UHI phenomenon on urban quality of life, particularly in north-western neighbourhoods and small pocket areas in the south and southeast. To mitigate the effect of UHI, the following strategies are recommended which include: increasing tree and vegetative cover, installing green roofs, installing cool, reflective roofs and using cool pavements (either reflective or permeable). In general, urban greening can significantly mitigate the UHI effect, both directly and indirectly, resulting in the decrease of air temperature and mean radiant temperature. It is therefore important for the city to strengthen and expand the hitherto stated UHI mitigation strategies to maintain quality urban life for Abuja city residents.

References

Abuja Facts (2015) Capital Facts for Abuja, Nigeria. Available online at: http://capitalcitymagazine. Blogspot.com /2015/03/abuja-facts.html.

Adeyeri, O. E**.**, Okogbue, E. C, Ige, S. O. and Ishola, K. A. (2015). *Estimating the Land Surface Temperature over Abuja using Different Landsat sensors* in Proceedings of climate change, environmental challenges and sustainable development (pp. 305-310). ISBN 978-978-53811-9-1. Available online at: *https://www.researchgate.net/publication/315707126*.

Alfraihat, R., Mulugeta, G. and Gala, T. S. (2016). Ecological Evaluation of Urban Heat Island in Chicago City, USA. *Journal of Atmospheric Pollution*, 4(1): 23-29. doi: 10.12691/jap-4-1-3.

Aljazeera (2019, March 6). Nigeria suffers severe heatwave with no relief in sight. *Aljazeera News*. Retrieved from https://www.aljazeera.com/news/2019/04/nigeria-suffers-severe-heatwave-relief-sight-190406085524415.html.

Amiri, R., Weng, Q., Alimohammadi, A. and Alavipanah, S. K. (2009). Spatial–temporal dynamics of land surface temperature in relation to fractional vegetation cover and land use/cover in the Tabriz urban area, Iran. *Remote Sens. Environ.,* 113(12): 2606–2617.

Asgarian, A., Amiri, B. J. and Sakieh, Y. (2015). Assessing the effect of green cover spatial patterns on urban land surface temperature using landscape metrics approach. *Urban Ecosystem,* 18: 209–222. https://doi.org/10.1007/s11252-014-0387-7.

Avdan, U. and Jovanovska, G. (2016). Algorithm for Automated Mapping of Land Surface Temperature Using LANDSAT 8 Satellite Data. *Journal of Sensors, 2016* (1480307). doi:10.1155/2016/1480307.

Balogun, O. (2001). *The Federal Capital Territory of Nigeria: Geography of Its Development*. University Press, Ibadan.

Buyantuyev, A. and Wu, J. (2010). Urban heat islands and landscape heterogeneity: linking spatiotemporal variations in surface temperatures to land-cover and socioeconomic patterns. *Landscape Ecol.*, 25:17–33. https://doi.org/10.1007/s10980-009-9402-4.

Chen, X. L., Zhao, H., Li, P. X. and Yin, Z. Y. (2006). Remote sensing image-based analysis of the relationship between urban heat island and land use/cover changes. *Remote Sensing of Environment, 104*: 133-146.

Della-Marta, P. M., Haylock, M. R., Luterbacher, J. and Wanner, H. D. (2017). Length of Western European Summer Heat Waves Since 1880. *J. Geophys. Res. Atmos., 112,* doi: 10.1029/2007JD008510.

Gago, E. J., Roldan, J., Pacheco-Torres, R. and Ordóñez, J. (2013). The city and urban heat islands: A review of strategies to mitigate adverse effects, *Renewable and Sustainable Energy Reviews*, 25: 749-758.

Gallo, K. P. and Owen, T. W. (1998). Assessment of urban heat islands: A multi sensor perspective for the Dallas Ft Worth, USA region. *Geocarto International, 13*: 35-41.

Gillespie, A. R., Rokugawa, S., Matsunaga, T., Cothern, J. S., Hook, S. J. and Kahle, A. B. (1998). Temperature and emissivity separation algorithm for advanced spaceborne thermal emission and reflection radiometer (ASTER) images. *IEEE Trans. Geosci. Remote Sens., 36*: 1113-1126.

Gray, K. A. and Finster, M. E. (2000). *The Urban Heat Island, Photochemical Smog, and Chicago: Local Features and the Problem and Solution. Northeastern University, Evanston, IL.*, Available online at: http://www.epa.gov/hiri/resources/pdf/post_chicago/chicago_toc_exsum.pdf.

Guha, S., Govil, H. and Mukherjee, S. (2017). Dynamic analysis and ecological evaluation of urban heat islands in Raipur city, India. *Journal of Applied Remote Sensing*, 11(3): 036020. doi: 10.1117/1.JRS.11.036020.

Huang, Q. and Lu, Y. (2018). Urban Heat Island Research from 1991 to 2015: A Bibliometric Analysis. *Theor. Appl. Climatol.*, *131*, 1055–1067.

Isioye, O. A., Akomolafe E. A., Abubakar A. Z., Aliyu O. A. and Maiwayo, T. (2019). *Geospatial Analysis of Urban Heat Island over Bauchi Metropolis and its Environs.* In Proceedings of the 1st International Conference of Engineering and Environmental Sciences (ICEES), Osun State University (UNIOSUN), Osogbo, Nigeria, 5-7 November 2019; pp. 655-669.

Jenerette, G., Harlan, S. and Brazel, A. (2007). Regional relationships between surface temperature, vegetation, and human settlement in a rapidly urbanizing ecosystem. *Landscape Ecol.*, 22:353–365. https://doi.org/10.1007/s10980-006-9032-z.

Jimenez-Munoz, J. C. and Sobrino, J. A. (2003). A generalized single-channel method for retrieving land surface temperature from remote sensing data. *J. Geophys. Res.*, *108*: 4688-4694.

Jinadu, A. M. (2004). Urban expansion and physical development problem in Abuja: implications. *Remote Sens. Environ.*, 104: 211–225.

Landsat Project Science Office. (2016). Landsat 8 science data user's handbook. Retrieved 13 September 2016, from https://landsat.usgs.gov/documents/Landsat8DataUsersHandbook.pdf. Accessed 13 May 2019.

Li, H. and Liu, Q. (2010). Comparison of NDBI and NDVI as indicators of surface urban heat island effect in MODIS imagery. *International Conference on Earth Observation Data Processing and Analysis (ICEODPA)*, *7285*(728503).

Lia, Z. L., Ning Wanga, H. W., Qiub, S., Sobrinod, J. A., Wane, Z., Tanga, B. H. and Yanf, G. (2013). Land surface emissivity retrieval from satellite data. *International Journal of Remote Sensing*, *34*(9-10): 3084-3127.

Liu, L. and Zhang, Y. (2011). Urban Heat Island Analysis Using the Landsat TM Data and ASTER Data: A Case Study in Hong Kong, *Remote Sens*., *3*: 1535-1552.

Mackey, C. W., Lee, X., and Smith, R. B. (2012). Remotely sensing the cooling effects of city scale efforts to reduce urban heat island. *Building and Environment*, *49*:348-358.

National Population Commission (NPC) (2006). The Nigeria Population Census, 2006. Available online at: http://www.population.gov.ng/index.php?option=com_content&view=artide&id=89.

Oleson, K. W., Monaghan, A., Wilhelmi, O., Barlage, M., Brunsell, N., Feddema, J. and Hu L. D. (2005). Interactions between urbanization, heat stress, and climate change, *Climatic Change*, *129*(3): 525-541.

Qin, Z., Zhang, M., Amon, K. and Pedro, B. (2001). Mono-window Algorithm for retrieving land surface temperature from Landsat TM 6 data. *Acta Geogr. Sinica*, *56*:456-466.

Song, C., Woodcok, C. E., Seto, K. C., Lenney, M. P., and Macomber, S. A. (2001). Classification and Change Detection Using Landsat TM Data: When and How to Correct Atmospheric Effects? *Remote Sensing of Environment*, *75*: 230-244.

Sun, Q., Tan, J. and Xu, Y. (2010). An ERDAS image processing method for retrieving LST and describing urban heat evolution: A case study in the Pearl River Delta Region in South China. *Environ. Earth Sci.*, *59:*1047-1055.

U.S. EPA Urban Heat Island Project (2002). Profile of Chicago, Available at URL: http://epa.gov/heatisl /pilot /archies/ chicago.pdf.

World Urbanization Prospects (2019). *United Nations Department of Economic and Social Affairs/Population Division*. Department of Economic and Social Affairs Population Division.

Zha, Y., Gao, J. and Ni, S. (2005). Use of normalized difference built-up index in automatically mapping urban areas from TM imagery. *International Journal of Remote Sensing, 24*:583–594.

Zhang, H. Z., Ye, Q., Cai X., Ma, Y. and Chen, M. (2013). Analysis of land use/land cover change, population shift, and their effects on spatiotemporal patterns of urban heat islands in metropolitan Shanghai, China. *Applied Geography, 44*:121-133.

Zhang, Y. (2006). Land surface temperature retrieval from CBERS-02 IRMSS thermal infrared data and its applications in quantitative analysis of urban heat island effect. *Journal of Remote Sensing,* 10:789-797.

Zhou, W., Qian, Y. and Li, X. (2014). Relationships between land cover and the surface urban heat island: seasonal variability and effects of spatial and thematic resolution of land cover data on predicting land surface temperatures. *Landscape Ecol.,* 29**:**153–167. https://doi.org/10.1007/s10980-013-9950-5.